

Analysis of welded thin-walled profiles under large deformations

Jiří Jankovec¹

Abstract: Axial collapse is one of the main structural deformation modes occurring in vehicle collisions and producing large deformation of the structure. Three different types of thin-walled rectangular tube specimens made of steel were investigated experimentally and numerically under axial compression in this paper. These investigations were made to assess the necessity to model the weld in the thin-walled structure undergoing large deformation.

Keywords: Thin-walled structure, Large deformation, Weld

1. Introduction

Light-weight structures of many different vehicle types (e.g. automobiles, rail vehicles) are often designed using thin-walled structures. The thin-walled elements are connected mostly using the weld connections. The design of new vehicles takes into account also the collision scenarios and thin-walled structures are used frequently for the energy absorption. There is a question, how the presence of a weld in the thin-walled tube influences (degrades or improves) the deformation characteristics of the structures in case of an impact or a collision. Therefore, the thin-walled structures with welds were studied in case of large deformation at the Computer Modelling Department of SKODA VYZKUM.

One of the mostly investigated deformation modes of a thin-walled structure is, besides the bending, the axial collapse of a thin-walled tube. Axial Collapse occurs usually in energy absorbing structures during direct frontal or rear or slightly off-angle impacts. The problem of rectangular tube axial collapse was investigated already analytically and numerically in many publications (e.g. [1-3] and [4]), and in this paper the investigations are expanded by inclusion of weld presence in the analyzed thin-walled rectangular tube specimen.

Three different types of thin-walled rectangular tube specimens were investigated experimentally and then numerically using the explicit finite element code LS-DYNA [5]. The behaviour of experiments and numerical models under axial compression will be compared at the end of this paper.

¹ Ing. Ph.D. Jiří Jankovec; SKODA VYZKUM; Tyllova 1/57, 31600 Plzeň, Czech Republic;
jiri.jankovec@skodavyzkum.cz

2. Description of thin-walled specimens

The following three thin-walled rectangular tube specimens of global dimensions 60x40x140 mm were studied under axial compression:

specimen 1-1 Rectangular tube specimen - basic

specimen 4-1 Rectangular tube specimen - with circular crush initiator holes

specimen 12-3 Rectangular tube specimen - with circular crush initiator holes and with fillet welds

These specimens are depicted in Fig. 1.

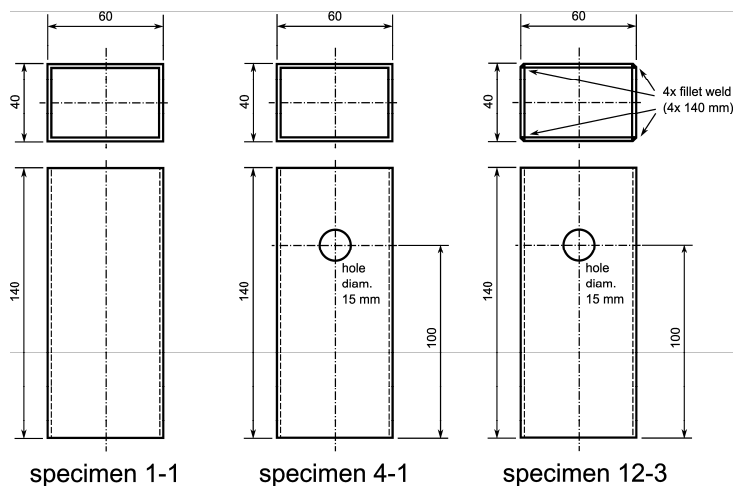


Fig. 1. Dimensions and shape of the rectangular tube specimens.

The rectangular specimens have the same wall thickness equal to 2 mm and they all are made of steel ČSN 11373. The third specimen (12-3) was welded using semiautomatic metal active gas (MAG) welding process. This specimen contains four fillet welds along its edges.

3. Experimental work

3.1. Description of the experiment

The rectangular tube specimens were placed between two thick steel plates positioned on the jaws of the hydraulic testing machine Zwick Z250 (in the Mechanical testing laboratory of SKODA VYZKUM) and they were compressed with the lower jaw movement velocity set to 500 mm/min. The upper jaw of the testing machine was fixed during these experiments. The maximal stroke of the lower jaw was set to 80 mm.

3.2. Results of the performed experiments

The deformation sequences during the axial compression progress are shown for each specimen in Fig. 2 to Fig. 4.

The load-displacement curves for each specimen were obtained automatically from the control and data acquisition units of the testing machine. These curves were used later for comparison with the curves obtained from the numerical simulation.

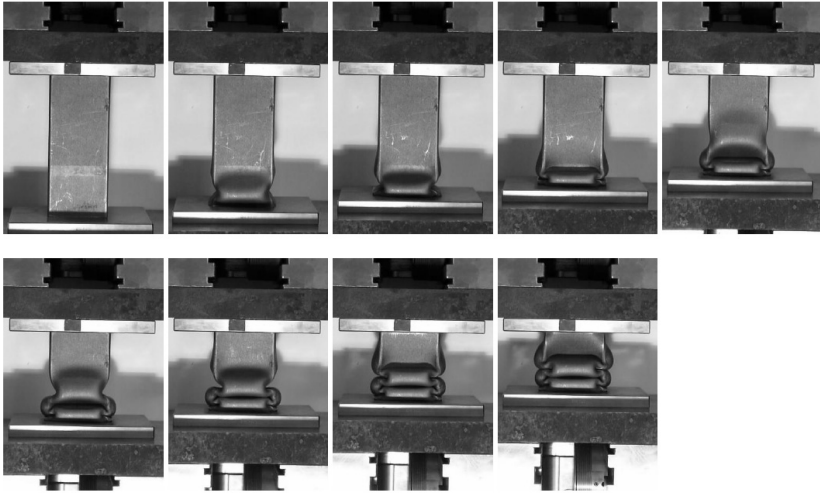


Fig. 2. Deformation sequence of specimen 1-1.

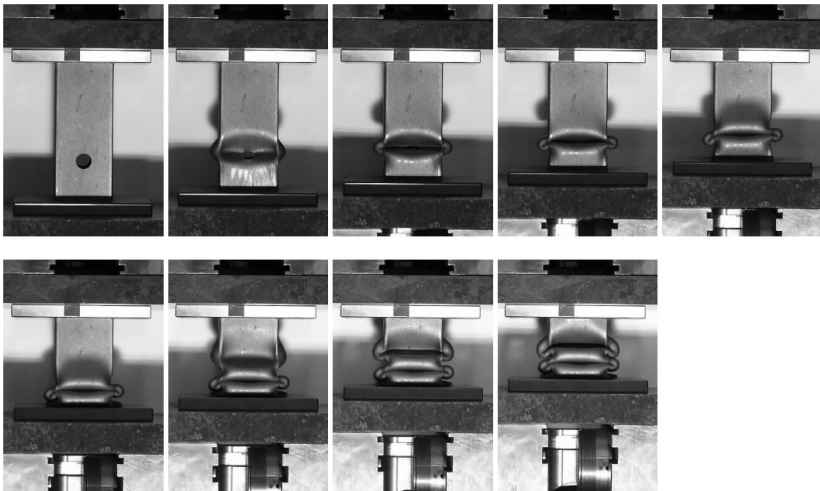


Fig. 3. Deformation sequence of specimen 4-1.

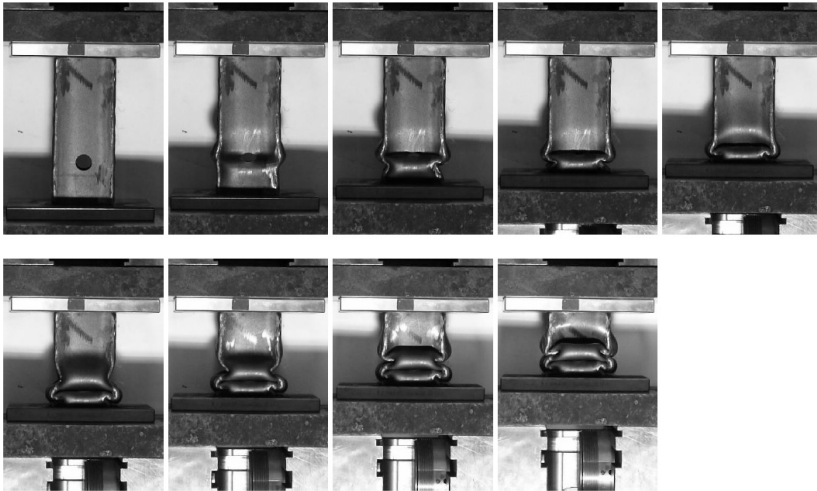


Fig. 4. Deformation sequence of specimen 12-3.

The specimen containing weld (12-3) exhibits no weld damage after the experiment.

4. Numerical simulations

4.1. Description of the numerical simulations

The pre-/post- processor LSPrePost was used to prepare finite element model of rectangular specimens for the simulation of the axial compression using finite element code LS-DYNA. The specimen was modelled as thin-walled structure using shell elements, defined using LS-DYNA keyword `*SECTION_SHELL`, using the element formulation of Belytschko-Tsai type. The thickness of the specimen elements was set to 2 mm. Five through thickness integration points was used in the model.

Material properties of the specimen were defined using keyword `*MAT_PIECEWISE_LINEAR_PLASTICITY` and its parameters were obtained from the tensile tests of the basic material of the specimen tube.

Two solid blocks were used to model the supporting plates, one under the specimen and second above the specimen. These blocks were modelled using solid elements using keyword `*ELEMENT_SOLID`.

Contact interface between the specimen and supporting plates was defined using keyword `*CONTACT_AUTOMATIC_NODES_TO_SURFACE`. Contact between elements of the specimen was modelled using keyword `*CONTACT_AUTOMATIC_SINGLE_SURFACE`.

The following boundary conditions were defined. Nodes on the top surface of upper supporting plate were fixed in vertical direction. The nodes on the bottom

surface of lower supporting plate have prescribed motion using defined velocity. The axial compression was modelled as a dynamical process with the prescribed compression 80 mm in 80 ms.

The model of specimen 4-1 includes two circular holes in the mesh. The model of specimen 12-3 contains welds modelled using keyword *CONSTRAINED_GENERALIZED_WELD_FILLET with the parameters corresponding to the geometry of the current fillet weld. Additionally the thickness of shell elements in the neighbourhood of the weld was set to 2.5 mm to model the local increase of the stiffness as a consequence of weld presence in the structure.

In the following figure (Fig. 5) the finite element model for each specimen is shown.

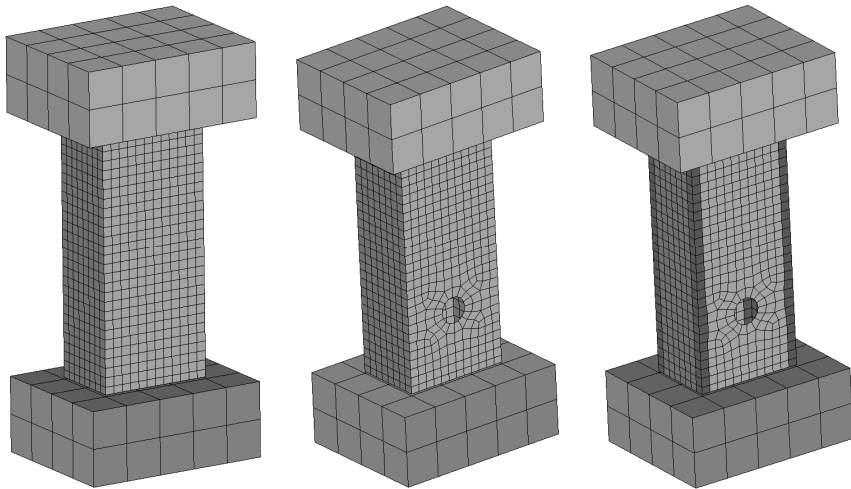


Fig. 5. Finite element model of axial compression for specimen 1-1, specimen 4-1 and specimen 12-3 (from left to right).

4.2. Results of the performed numerical simulations

The deformation sequences during the axial compression progress obtained from numerical simulation are shown for each specimen in Fig. 6 to Fig. 8.

The load-displacement curves obtained from the simulation will be compared with the curves from experiment.

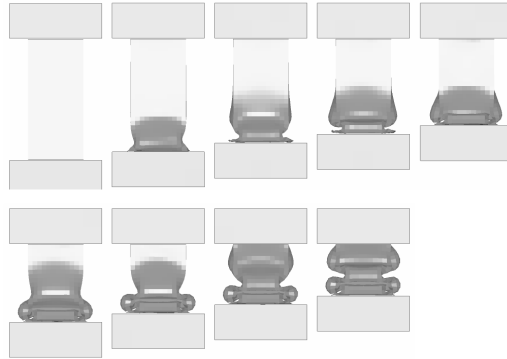


Fig. 6. Deformation sequence from numerical simulation for specimen 1-1.

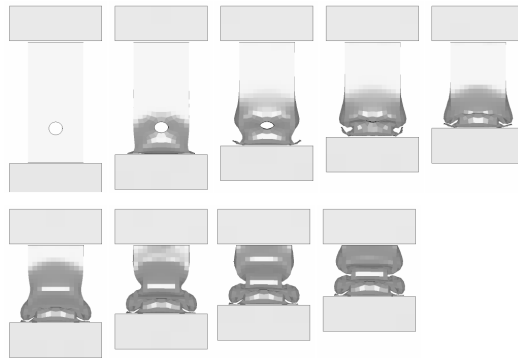


Fig. 7. Deformation sequence from numerical simulation for specimen 4-1.

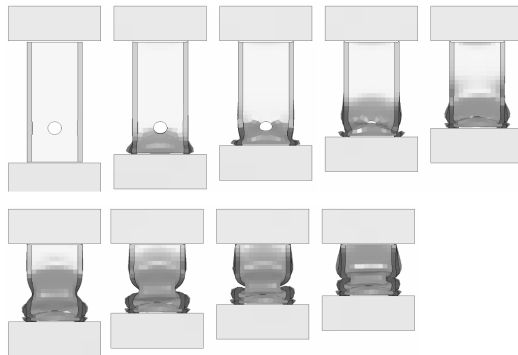


Fig. 8. Deformation sequence from numerical simulation for specimen 12-3.

5. Comparison of results

Comparison of load-displacement curves from experiment and simulation is shown in Fig. 9 for each specimen type. It yields from these graphs that the occurrence of local extremes is well corresponding in case of specimen 1-1. The timing of local extreme occurrence differs in case of specimens 4-1 and 12-3. Integrating the load-displacement curves the *Total absorbed energy* of each specimen can be obtained.

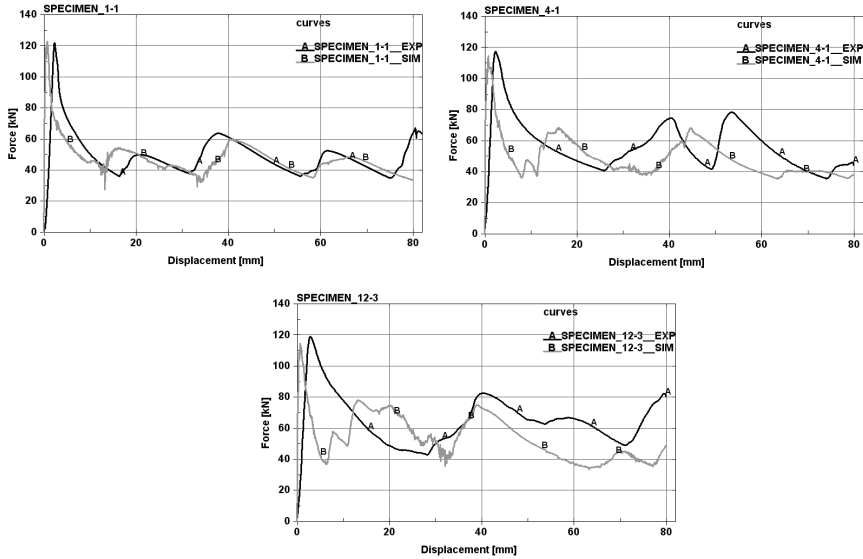


Fig. 9. Comparison of load-displacement curves.

The values of *Maximal force* transmitted through each specimen and the values of *Total absorbed energy* are shown in Tab. 1.

Table 1. Maximal force and Total absorbed energy

	Maximal force	Total absorbed energy
Specimen 1-1	$F_{\text{exp}} = 122$ [kN]	$E_{\text{exp}} = 3920$ [J]
	$F_{\text{sim}} = 123$ [kN]	$E_{\text{sim}} = 3800$ [J]
Specimen 4-1	$F_{\text{exp}} = 118$ [kN]	$E_{\text{exp}} = 4530$ [J]
	$F_{\text{sim}} = 115$ [kN]	$E_{\text{sim}} = 3940$ [J]
Specimen 12-3	$F_{\text{exp}} = 119$ [kN]	$E_{\text{exp}} = 5200$ [J]
	$F_{\text{sim}} = 115$ [kN]	$E_{\text{sim}} = 4340$ [J]

From the values in the above mentioned table the following conclusions results:

The values of *Maximal force* for experiment and simulation are very close each other in case of specimen 1-1.

In case of specimens with the circular-hole initiator (4-1 and 12-3) the *Maximal force* has decreased in relation to the basic specimen, as expected, and the *Total absorbed energy* has increased in relation to the basic specimen, as non-expected.

The specimens containing circular-hole initiator (without and with the weld) have very similar values of the *Maximal force* - it means that this value is not depending on the weld presence.

The specimen containing weld has absorbed higher amount of energy during the 80 mm compression than the specimens without the weld.

It has to be noted that the above mentioned conclusions correspond to the actual weld location and orientation and to the specimen shape used in this investigation.

6. Summary/Conclusion

In this paper three different thin-walled rectangular tube specimens under axial compression were investigated experimentally and numerically. The specimens differing in circular-hole initiator presence and in weld presence were compared from the point of Maximal force and Total absorbed energy view.

Acknowledgements

The paper has originated in the framework of solving the Research Plan of the Ministry of Education, Youth and Sports of the Czech Republic MSM4771868401.

References

- [1] Ohokubo Y., Akamatsu T. and Shirasawa K., "Mean Crushing Strength of Closed-Hat Section Members," SAE Paper No. 740040 (Society of Automotive Engineers, Feb. 1974).
- [2] Johnson W., Soden P.D. and Al-Hassani S.T.S., "Inextensional Collapse of Thin-Walled Tubes Under Axial Compression," *Journal of Strain Analysis*, **12**(4), pp. 317-330 (1977). ISSN 0309-3247.
- [3] Wierzbicki T. and Abramowicz W., "On The Crushing Mechanics of Thin-Walled Structures," *Journal of Applied Mechanics*, **50**(4a), pp. 727-734 (1983). ISSN 0021-8936.
- [4] Mamalis A.G., Manolakos D.E., Spentzas K.N., Ioannidis M.B., Koutroubakis S. and Kostazos P.K., "The Effect of the Implementation of Circular Holes as Crush Initiators to the Crushing Characteristics of Mild Steel Square Tubes: Experimental and Numerical Simulation," *International Journal of Crashworthiness*, **14**(5), pp. 489-501 (2009). ISSN 1754-2111.
- [5] *LS-Dyna User's Manual ver. 971* (Livermore Software Technology Corporation (LSTC), 2007).